

Crash Test of an MD-500 Helicopter with a Deployable Energy Absorber Concept

J. D. Littell*, K. Jackson**, S. Kellas**

*ATK Space Systems, NASA Langley Research Center MS 495, 12 W. Bush Rd., Hampton, Virginia 23681,

**NASA Langley Research Center MS 495, 12 W. Bush Rd., Hampton, Virginia 23681

Abstract - On December 2, 2009, a full scale crash test was successfully conducted of a MD-500 helicopter at the NASA Langley Research Center Landing and Impact Research Facility . The purpose of this test was to evaluate a novel composite honeycomb deployable energy absorbing (DEA) concept for attenuation of structural and crew loads during helicopter crashes under realistic crash conditions. The DEA concept is an alternative to external airbags, and absorbs impact energy through crushing. In the test, the helicopter impacted the concrete surface with 11.83 m/s (38.8 ft/s) horizontal, 7.80 m/s (25.6 ft/s) vertical and 0.15 m/s (0.5 ft/s) lateral velocities; corresponding to a resultant velocity of 14.2 m/s (46.5 ft/s). The airframe and skid gear were instrumented with accelerometers and strain gages to determine structural integrity and load attenuation, while the skin of the airframe was covered with targets for use by photogrammetry to record gross vehicle motion before, during, and after the impact.

Along with the collection of airframe data, one Hybrid III 50th percentile anthropomorphic test device (ATD), two Hybrid II 50th percentile ATDs and a specialized human surrogate torso model (HSTM) occupant were seated in the airframe and instrumented for the collection of occupant loads. Resultant occupant data showed that by using the DEA, the loads on the Hybrid II and Hybrid III ATDs were in the “Low Risk” regime for the injury criteria, while structural data showed the airframe retained its structural integrity post crash. Preliminary results show that the DEA is a viable concept for the attenuation of impact loads.

INTRODUCTION

The Landing and Impact Research Facility (LandIR) at NASA Langley Research Center (LaRC) has a rich history of aircraft and spacecraft impact testing. Originally built in 1965 to train astronauts to land on the moon during the Apollo program [1], it has since been converted to the Impact Dynamics Research Facility (IDRF) for use as a full-scale aircraft crash test facility [2]. Since the mid 1970s, over 150 vehicles comprising a mix of general aviation aircraft, helicopters, and fuselage subsections have been tested at the recently renamed LandIR [3]. Currently, the facility supports NASA’s Constellation Program and the Subsonic Rotary Wing Crashworthiness Program for Orion crew module landing and rotorcraft impact testing, respectively.

Aircraft crashworthiness has mainly been focused on the attenuation of impact loads and ultimately the mitigation of occupant injury. Crushable structures such as subfloors [4-9] and energy absorbing seats [10] have been examined as possible internal attenuation devices. Concepts like these are used in current aircraft fleets; however, the minimal volume inside the aircraft cabin limits their effectiveness. External deployable energy absorbers do not have the same constraints as the internal devices. Because they are stowed in a compacted state and deployed on command, they can have large external volumes in which to absorb energy. However, potential disadvantages include stowage requirements, deployment mechanisms that can require complex control systems and hardware, and the added weight that can limit the performance characteristics of the aircraft.

External energy absorbing airbag concepts have been evaluated for crash attenuation [11-14] in the past. Similar to an automotive airbag system, these deploy immediately before impact and offer attenuation through active or passive venting systems. One design challenge with airbags is that large shear forces often developed from high horizontal velocities may cause them to fail. In addition, deficiencies in

venting, active control systems, and effectiveness on uneven terrain led researchers at NASA LaRC to consider an alternative method.

At NASA LaRC, a program has been implemented to demonstrate a novel Deployable Energy Absorbing (DEA) composite honeycomb concept [15-17]. Originally considered for evaluation on NASA's Orion spacecraft, the DEA's were then considered in civil aircraft as a potential device to attenuate crash loads and to alleviate occupant injuries. The DEA used for this test was fabricated from Kevlar/epoxy composite sheets, and then assembled to form the hexagonal cell walls. The flexible hinge design allows the entire structure to lie flat until deployed, at which point the cells form a honeycomb shape oriented normal to the airframe and impact surface. Through a systematic building block approach, the DEA's cell walls, materials and geometry have been studied by conducting tests and analyses at the material, component, and subscale level. The crash test of a MD-500 helicopter, described herein is a proof-of-concept test, which gives researchers a chance to validate the concept on an actual airframe under realistic crash conditions. Figure 1 shows an example DEA used in a subscale crush test. Note these photos do not depict the actual DEA used in the helicopter test.

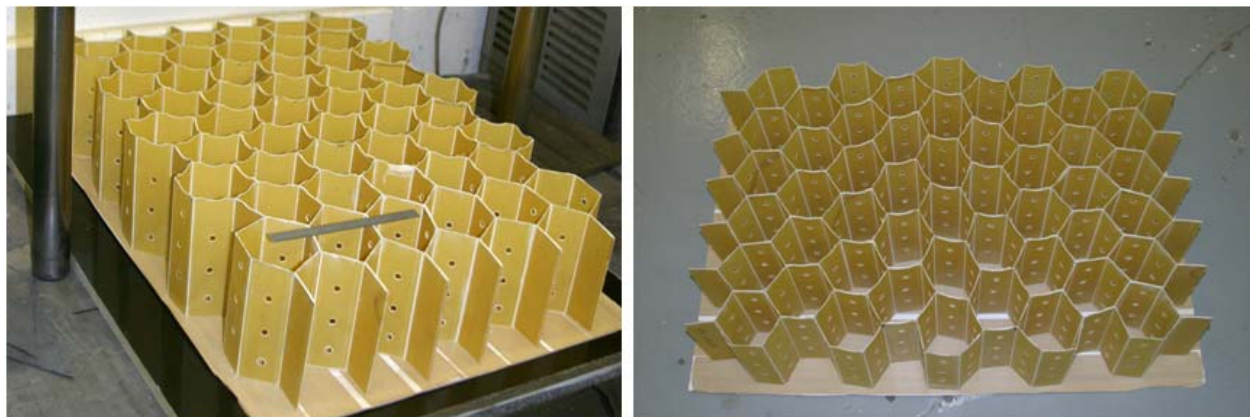


Figure 1 – An example DEA used in subscale testing. Isometric view (left) and top view (right).

TEST ARTICLE DESCRIPTION

The MD-500 and the MD-530 are derivatives of the Hughes OH-6 helicopter. Over 5,000 airframes have been built since 1982. The latest civilian utility variants are the MD-500E and the MD-530F. The military derivative of the helicopter is the Defender series that is currently in service in the U.S. Army. Currently, the MD-500E is used as a general-purpose utility and executive transport helicopter. The MD-500E helicopter is powered by a single Rolls Royce or Allison turbo shaft 250-C20B engine (420 hp). Maximum airspeed is 289 km/hr (156 knots), and the maximum gross weight is 1360 kg (3,000 lb), with an empty weight of 703 kg (1,550 lb.) The range is 556 km (300 nautical miles). The total length of the airframe is 9.4 m (30.84 ft), and the tail height is 2.71 m (8.9 ft.) [18].

The U.S. Army Mission Enhanced Little Bird program provided the MD-500 helicopter to LaRC. Components not included in the as-delivered helicopter were the engine, gear box, main rotor, rear tail and tail rotor, avionics, fuel tanks, seats, restraints and doors. Figure 2 shows the helicopter as delivered to NASA LaRC.



Figure 2 – As-delivered MD-500 helicopter.

Further modifications were necessary to prepare the MD-500 helicopter for the test. A summary of the major modifications completed is as follows:

- 1 – Damaged aluminum skin near helicopter tie down points and acrylic windshield panels were replaced or repaired.
- 2 – Original oleo-pneumatic skid gear struts were replaced with crushable energy absorbing struts.
- 3 – Four layers of 0.25 mm (0.010 in) thick graphic/epoxy fabric were added to the belly to enhance the load carrying capability due to the expected loading from the DEA crushing.
- 4 – Aluminum straps were added to each side of the helicopter at the exterior water line which served as DEA tie down attachment points.
- 5 – Box beams were added to the front and rear bulkheads to serve as LandIR cabling system attachment points used for lifting and releasing.
- 6 – Original skid gear was replaced with new gear.

Ballast mass was added to the main rotor, engine, tail, fuel tank and avionics areas to achieve the desired take-off weight of 1329 kg (2930 lbs) and to place the overall center-of-gravity at a realistic location. Standard military replacement seats were purchased and installed in the helicopter.

Four simulated human occupants were seated in the aircraft. The pilot (front left) was a standard 50th percentile Hybrid III Anthropomorphic Test Device (ATD). The co-pilot (front right) and rear passenger (rear right) were 50th percentile Hybrid II ATDs. The other rear passenger (rear left) was a specially designed human surrogate torso model (HSTM), designed to measure the internal loads on a human torso [19].

The helicopter was instrumented to collect 160 channels of airframe and ATD occupant response data. Accelerometers were placed on critical components of the airframe and added ballast locations, while strain gages were placed on the bulkheads, keel beam, and skid gear. Seventeen white/black photogrammetric targets were placed on the left side of the vehicle, and used to collect impact conditions and gross vehicle motion before, during- and after impact. The rear tail structure was painted with a white/black dot pattern for a full-field strain proof-of-concept photogrammetric analysis.

The DEAs were designed and fabricated in-house at NASA LaRC. Two DEA configurations were used for the test; one for the front and one for the rear of the helicopter, as shown in Figure 3. Previously

conducted analyses [20] showed the maximum energy attenuation configuration for this test's combined velocity conditions was with both DEAs canted 20 degrees forward. However, geometric limitations of the airframe required that the rear DEA remain purely vertical. The DEAs were attached in a pre-deployed configuration. (They are designed to be stowed flat underneath the airframe and deploy only in the event of a crash.) For more on the deployment mechanisms considered, see Ref [9]. The deployed DEA blocks are tied to the previously mentioned aluminum straps with nylon cords.

The height of the front DEA was approximately 55.25 cm (21.75 in), and the width was 67.82 cm (26 in) on the end against the helicopter and 83.3 cm (32.8 in) on the free end. The front DEA covered approximately 82.3 cm (32.4 in) longitudinal distance of the helicopter and was fastened approximately between stations 44 and 78.50. For reference, the tip of the helicopter's nose is at station 15. There was approximately 17.8 cm (7 in) vertical clearance between the forward free end and the ground and approximately 10.2 cm (4 in) vertical clearance between the rearward free end and the ground.

The height of the rear DEA was approximately 46.7 cm (18.4 in), and it was 57.66 cm (22.7 in) wide on the end against the helicopter and 76.2 cm (30 in) on the free end. The rear DEA covered approximately 81.2 cm (32 in) longitudinal distance of the helicopter and was fastened between stations 100 and 130. There was 12.1 cm (4.75 in) of clearance between the front end and the ground and 7.6 cm (3 in) of clearance between the rear end and the ground. The specific height of both DEAs was intended to allow the skid gear to contact first, stabilizing the helicopter, and then the DEA's would subsequently attenuate the impact load. The combined weight of the front and rear DEAs was 14.42 kg (31.8 lbs).



Figure 3 – Front (left) and Rear (right) DEA's fitted on the MD-500 helicopter.

The nominal helicopter impact conditions were 12.19 m/s (40 ft/s) horizontal velocity and 7.92 m/s (26 ft/s) vertical velocity, giving a resultant velocity of 14.54 m/s (47.7 ft/s) at a 33 degree glide angle. The impact surface was concrete. The particular velocity condition was chosen to represent a severe, but survivable crash, and not explicitly based on a particular standard such as MIL-STD-1290A [21]. The nominal impact velocity is achieved by swinging the helicopter through two sets of parallel swing cables, located on either side of the vehicle. A separate set of pullback cables lifts the vehicle to the specified drop height. A set of pyrotechnic cutters severs the pullback cables, allowing the vehicle to swing toward the ground via the swing cables. Immediately before impact, pyrotechnic cutters sever the swing cables such that the vehicle is in free fall. A picture of the MD-500 helicopter in the test configuration attached to LandIR cabling systems is shown in Figure 4. Wood supports between the skid gear and box beam cabling attachment structure are there for pretest support, and were removed prior to the test.

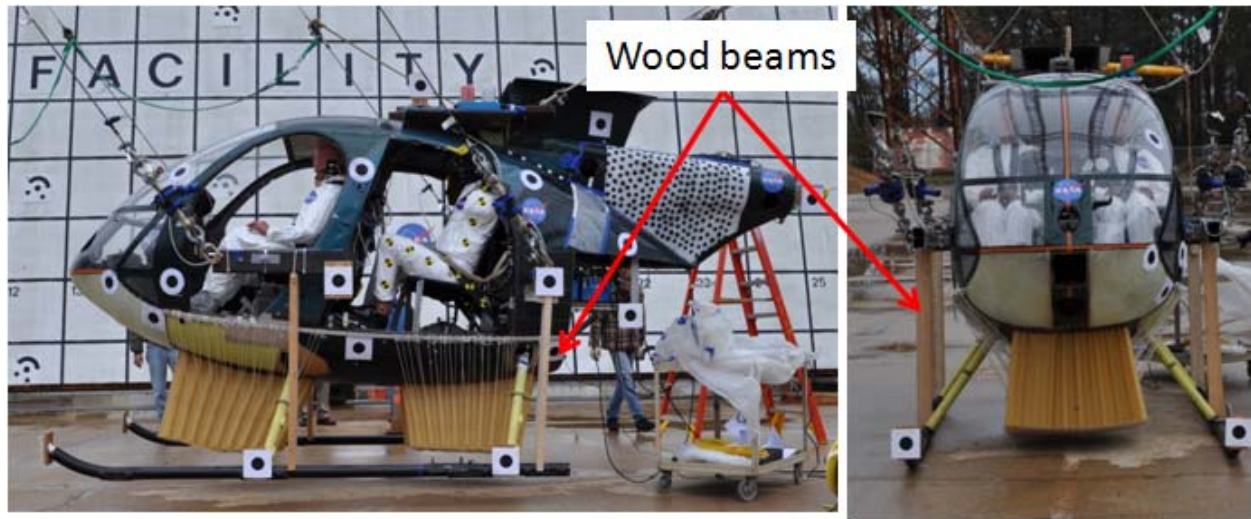


Figure 4 – MD-500 in test configuration. Side view (left) and front view (right).

RESULTS

External high speed cameras filming at 1000 frames per second were used to capture pre-, during-, and post- impact video. Helicopter impact conditions, as determined from the photogrammetry analysis, were 11.8 m/s (38.8 ft/s) forward and 7.8 m/s (25.6 ft/s) vertical velocities, 5.69 degrees pitch, 9.30 degrees yaw and 7.04 degrees roll with angular rates of 4.82 deg/s yaw and 1.11 deg/s roll. Figure 5 shows an image sequence through the impact obtained from the video capture.

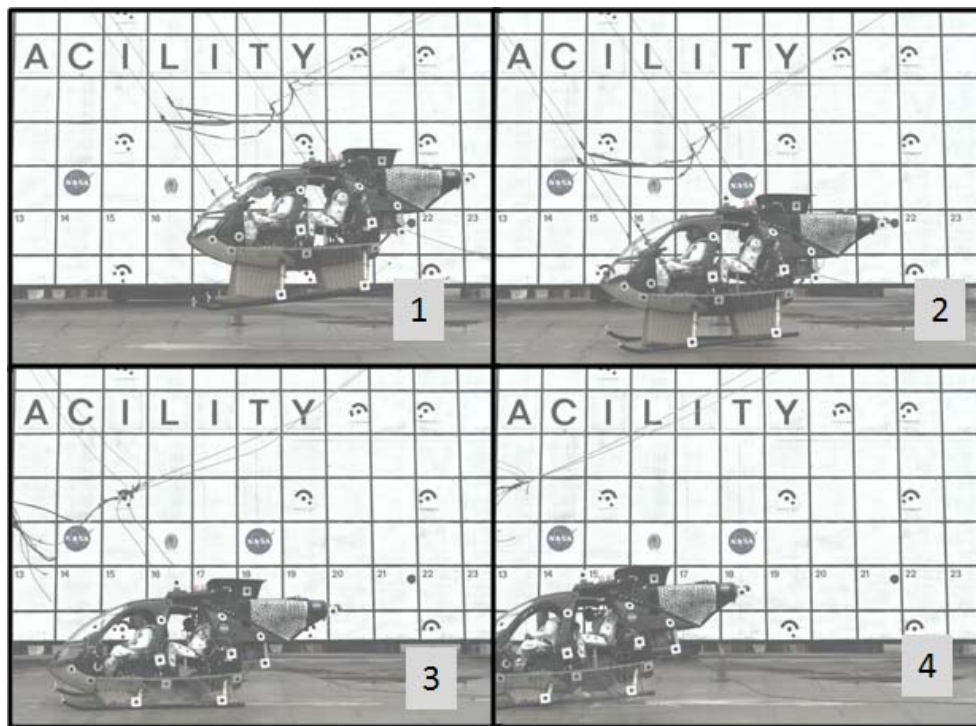


Figure 5 – Image sequence of impact.

In Figure 5, picture 1 (upper left) shows the helicopter approximately 30 ms before impact, picture 2 (upper right) shows the helicopter at the point of first skid gear impact, picture 3 (lower left) shows the point of maximum DEA crushing, and picture 4 (lower right) shows a post-impact rebound. The front-right side skid gear is seen to impact the ground first, which was caused by the yaw and roll present in the swing. At the point of maximum crush deflection (picture 3), the helicopter has straightened out to show almost no pitch. After the point of maximum crush, the nose is seen to pitch forward on the rebound, presumably due to friction between the DEA and the impact surface. The vehicle came to rest approximately 13.72 m (45 ft) from the impact location.

Onboard cameras filming at 24 frames per second were used to capture the motion of the occupants before-, during-, and post-impact. In Figure 6, images 1 to 4 show a sequence from a forward facing camera mounted on the center bulkhead on the co-pilot side of the helicopter.



Figure 6 – Image sequence of impact viewed from an onboard camera.

The back of the co-pilot ATD's head is in the right of each picture, while the avionics panel is in the lower left. The instrumentation cable is seen emanating from the back of the co-pilot's head. Picture 1 (upper left) in Figure 6 shows the vehicle resting at the drop height, before release. Picture 2 shows the vehicle midway through the swing, in which the pitch down attitude can be seen by noting the difference in the angle of the impact surface between it and picture 1. Picture 3 shows the vehicle as the DEA is crushing; when the vehicle has leveled to approximately zero pitch. Picture 4 shows the vehicle at rest after the impact. The helicopter turned toward the left after the impact, causing the co-pilot's head to flail to the right. Also note that the head is further away from the camera in the post-test image, indicating that the co-pilot ATD also lunged forward before being stopped by the seat belt restraints.

Airframe Results

Figure 7 shows the airframe post-impact. The crushed DEAs can also be seen underneath the airframe.



Figure 7 – MD-500 helicopter in post-impact location.

Post-test inspection of the airframe showed very little damage on the main structural components of the airframe. The seats were also undamaged. The front airframe skin reacting against the forward DEA showed some minor buckling; however the large majority of the airframe's structure was undamaged. Figure 8 shows the co-pilot's side buckled subfloor, which reacted against the DEA crushing. Inside the circled portion is a buckled frame.

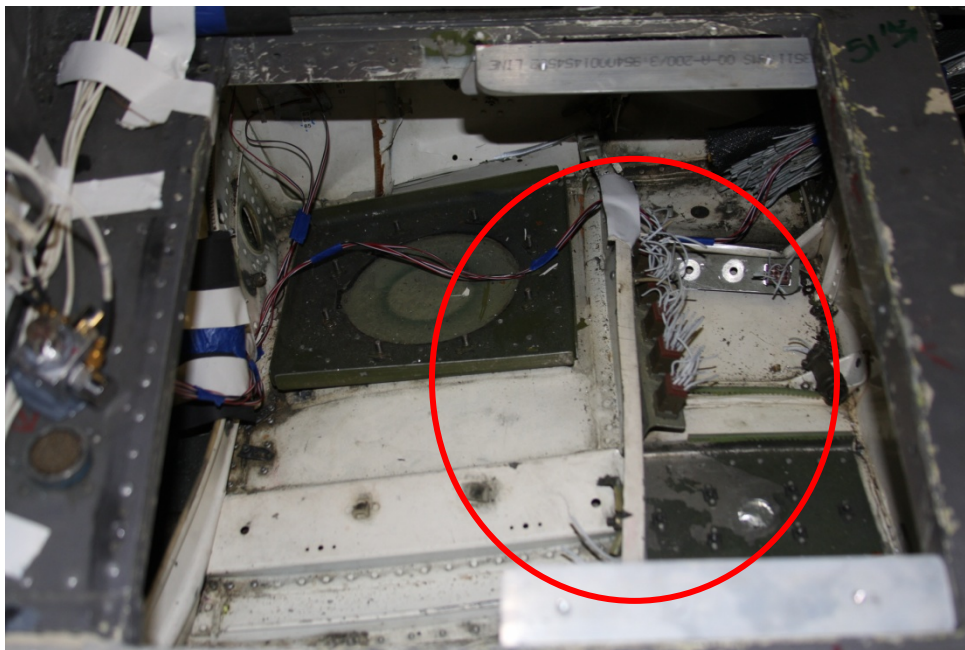


Figure 8 – Co-pilot subfloor and buckled frame.

The accelerations from various portions of the airframe were also examined. Figure 9 shows vertical accelerations from the rear floor, front bulkhead, and top ballast mass. The “rear floor” accelerometer was positioned centered beneath the rear ATD’s feet. The “Center B/H” accelerometer was placed on the lifting hardware attached to the center bulkhead, directly behind the front seats. The “Top Ballast” accelerometer was placed on the mounting plate where the rotor blades would be attached. The accelerations are filtered using a four pole, 60 Hz. lowpass digital Butterworth filter. Note that in all plots, impact time is at 0.205 sec.

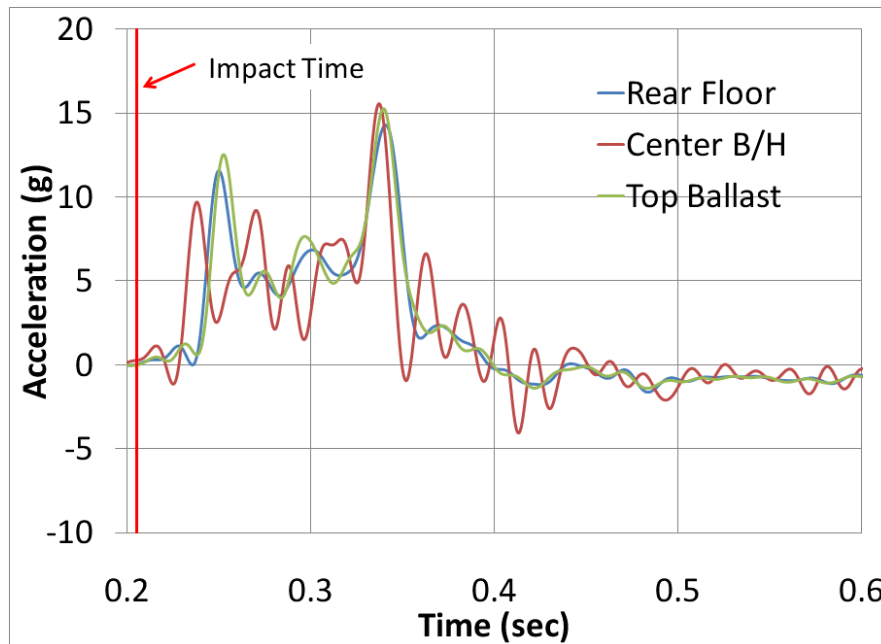


Figure 9 – Vertical accelerations from the airframe.

Figure 9 shows all three locations of vertical acceleration have generally the same response. Each has an initial spike at approximately 0.25 sec. Each then settles down to approximately 5 g and then spikes back up to 15 g around 0.35 sec. The first acceleration spike is attributed to the initial impact of the right front skid gear and the subsequent straightening of the vehicle before the DEA crush begins. The plateau between the spikes is the DEA crushing and absorbing the impact energy, while the 15 g spike near the end of the pulse is after the DEAs have reached their crush stroke limit. Horizontal accelerations are plotted next in Figure 10. The two accelerometers in Figure 10 are located on both the left and right side of the helicopter, on the floor and adjacent to the rear seat-to-floor attachment points.

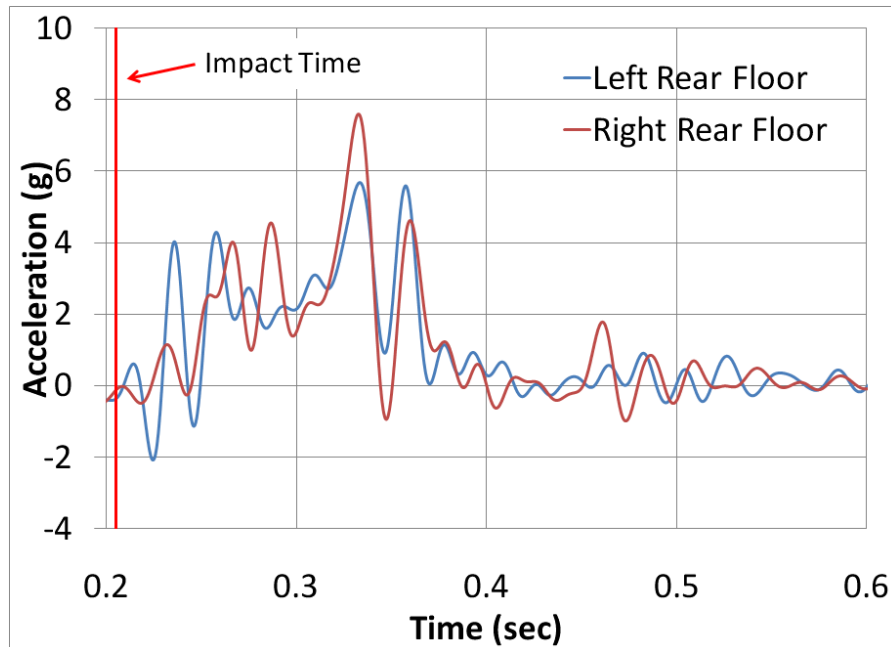


Figure 10 – Horizontal accelerations from the airframe.

The horizontal accelerations start to increase at approximately 0.2 sec, which is when the vehicle's front right skid gear reached the ground. The accelerations increase to approximately 7.6 g on the right and 5.7 g on the left side at approximately 0.33 sec, which is the point of maximum DEA contact, thus creating the largest frictional force between the DEA and ground. The right portion of the floor saw slightly higher accelerations, presumably from the fact that the right side of the vehicle impacted first.

Strains from the various structural members of the airframe were collected from strain gauge rosettes. Through strain transformation techniques and a modulus scaling factor, major and minor stress are plotted to determine post-impact structural integrity. On the skid gear, to assess the effect of bending strain, gages were placed inboard (toward the middle of the helicopter) and outboard (toward the outside of the helicopter) in pairs, and also placed forward (toward the front) and aft (toward the rear) in pairs. Representative plots are shown in Figure 11 for strains on a forward and aft location of the keel beam. Right front skid gear stresses are shown in Figure 12.

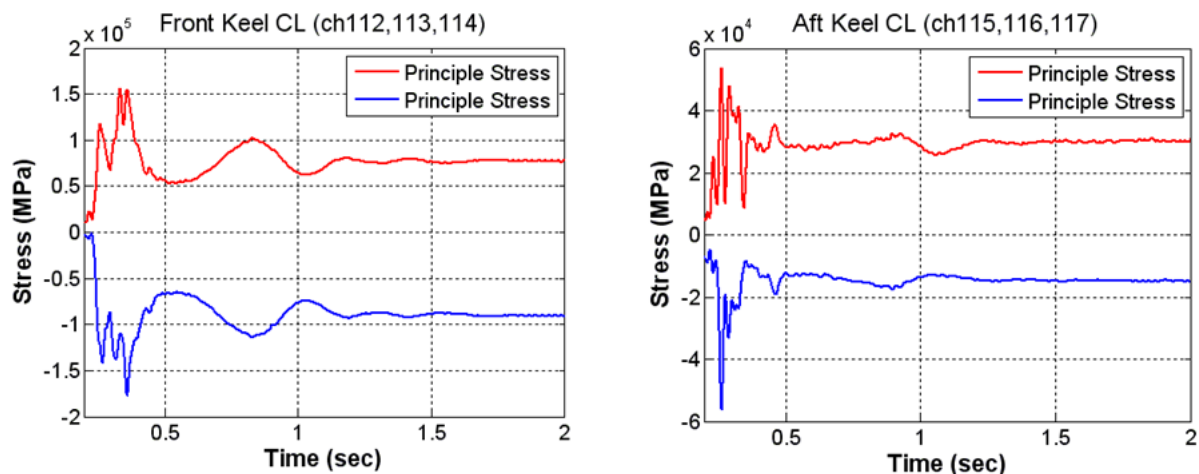


Figure 11 – Stresses on a forward (left) and aft (right) keel beam location.

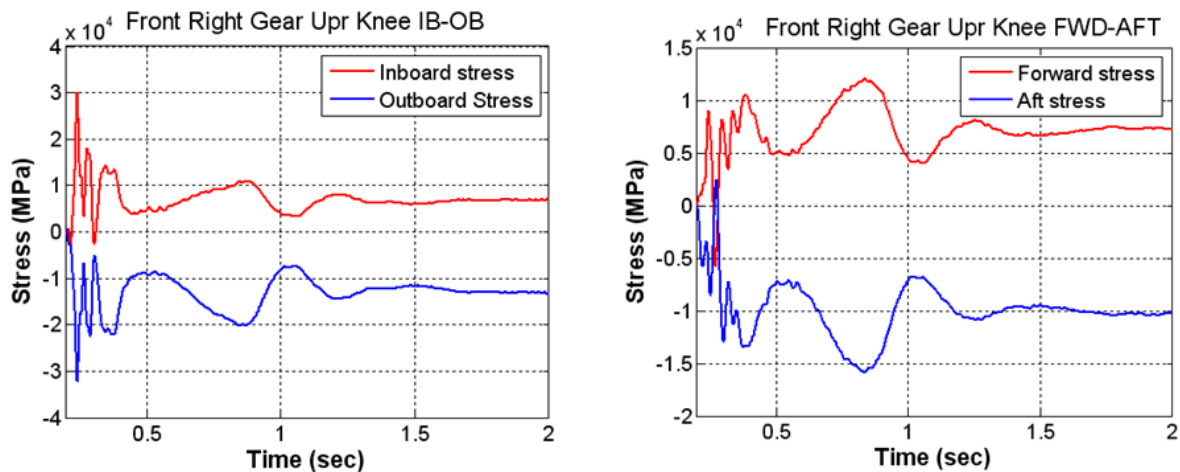


Figure 12 –Inboard and Outboard (left) and Forward and Aft (right) stresses on the front right skid gear.

All skid gear stresses were well within the elastic range for aluminum and showed no plastic deformation on the measured locations, which was 7.62 cm (3 in) above the curved “knee” of the skid gear. The right skid gear did exhibit some plastic deformation in areas which contacted the airframe structure which was higher than the left side, presumably because the helicopter impacted on the right side initially. However, no areas of either gear failed. This behavior was fortunate because the skid gears acted as outriggers and helped to stabilize the helicopter as it impacted and as the DEA crushed.

Occupant Responses

The instrumented ATDs were also examined to assess the risk of occupant injury. One of the main ways to assess occupant injury is to examine the loads measured from a load cell mounted in the lumbar region of each ATD and compare it to the established limits in FAR Part 27.562 (C) [22]. Lumbar loads from the occupants equipped with lumbar load cells are shown in Figure 13. Note the rear left HSTM did not have a lumbar load cell, and thus is not plotted in Figure 13.

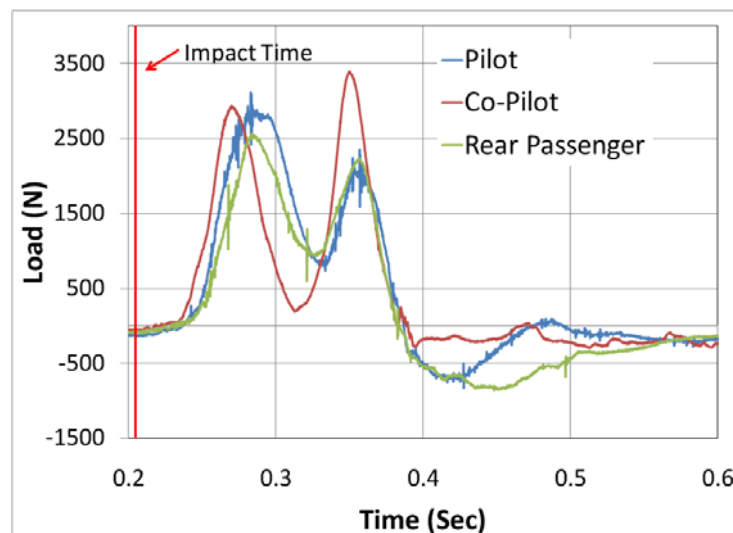


Figure 13 – Lumbar loads from three occupants.

Figure 13 shows that the maximum lumbar load occurred in the co-pilot, which was most likely due to the vehicle impact on the right side first. However, examining the plots, one can note that the general response is similar for all three occupants. There is an initial peak around 0.275 sec, which represents the dummies impacting against their seats. The plots then reach a relative minimum before they reach a second peak at approximately 0.35 sec. The peak load for all three plots was 3380 N (755 lbs). When evaluating potential for injury for a 50th percentile occupant, FAR Part 27.562 (c) establishes a lumbar limit of 6672 N (1,500 lbs) as being injurious. The loads incurred in the occupants were well below this limit.

The pilot, co-pilot, and rear passenger seat pan accelerations were input into the Brinkley model [23], which has been used to evaluate the risk of injury in a variety of aircraft and spacecraft systems [24-25]. The Brinkley model estimates the likelihood of injury using lumped parameter representation of the body for each axis (x – chest to back direction, y – sideways direction, and z – vertical or spinal direction) of the occupant. The coefficients of these lumped parameters in the mathematical formulation are based on experiments conducted on volunteers from the US armed forces. For more information on the development and use of the Brinkley model, see Reference 22.

Seat pan acceleration time history pulses in all three directions are input into the Brinkley model. The output result from the Brinkley model is the beta value, which is an index taking into account responses from all three axes. The Brinkley model also outputs dynamic response time histories of the occupant in all three axes. The value of beta is given for three risk categories (low, medium and high), and a beta value greater than one in a particular category pushes the injury probably into the next higher category.

Table 1 indicates that the probability of injury in the pilot, co-pilot or rear passenger is below the low category, indicating a very low probability of risk. Next, dynamic response time histories for each occupant were output from the Brinkley model, and Figure 14 shows both the seat pan accelerations and the Brinkley dynamic response.

Table 1 – Brinkley Beta results for low, medium and high limits

Beta	Pilot	Co-Pilot	Rear Passenger
Low	0.70	0.62	0.86
Medium	0.59	0.52	0.72
High	0.46	0.41	0.57

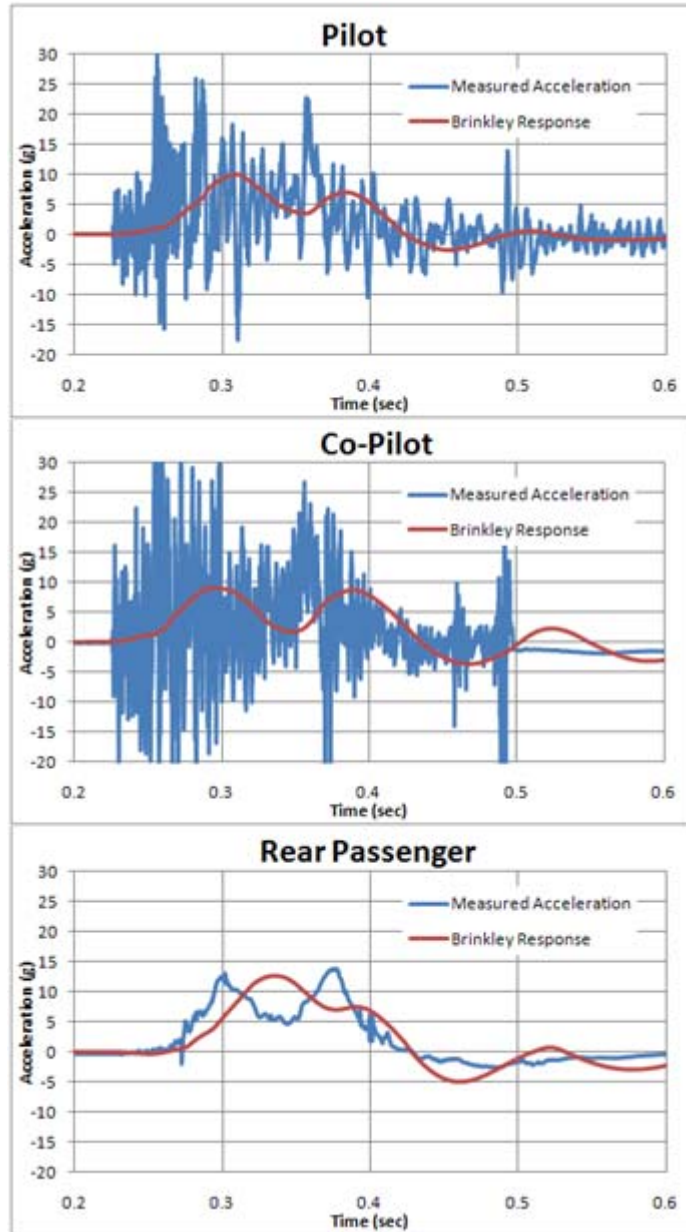


Figure 14 – Measured vertical seat pan time histories and dynamic response for each occupant from the Brinkley model.

The time histories shown in Figure 14 are the measured seat pan accelerations compared to the Brinkley responses for each occupant. Notice in the Brinkley responses, the front pilot and co-pilot have very similar time histories while the rear passenger is slightly different. This difference can be attributed to the differences in seats. The front pilot and co-pilot were in identical mesh bucket seats, while the rear passenger was in a mesh bench seat. The response data shows that the front occupants saw a 9-10 g dynamic response at 0.3 sec. These results, along with the beta value, show that there is a very low risk of injury to the occupants.

Photogrammetry Results

The photogrammetry system was used for motion tracking from the ground. High speed cameras filmed the left side of the helicopter at 1000 frames per second during the test and were able to collect approximately one second of data. The photogrammetry system provided all of the velocities and flight attitudes for the helicopter before-, during-, and post-impact. The impact velocities were obtained by averaging all of the data from the points before the impact during rigid body flight of the helicopter. Impact attitudes were computed by measuring digitally created lines and angles with a reference. For a full description on the photogrammetry system setups and techniques used see Reference 26. Time histories of the impact velocities and angles are shown in Figure 15.

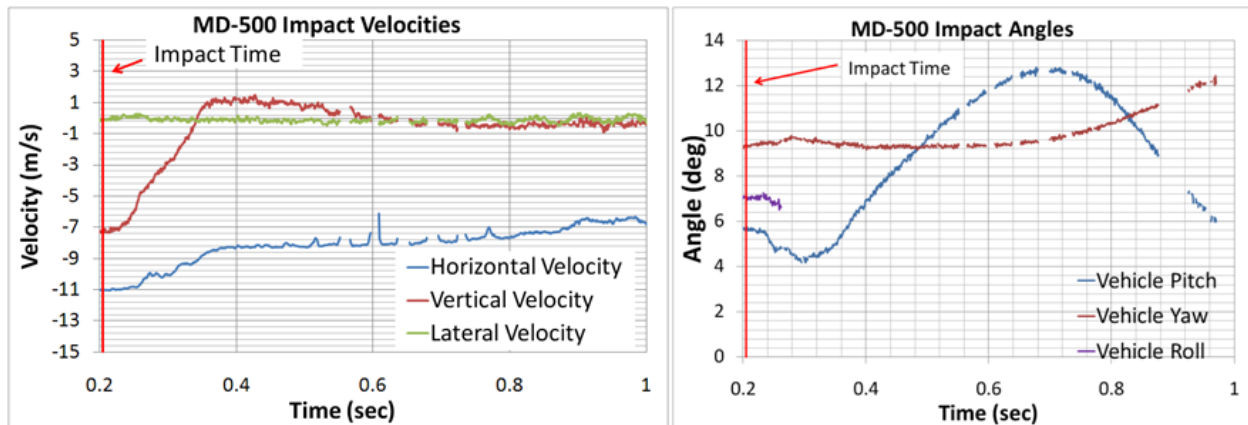


Figure 15 – Time histories of MD-500 velocities and angles.

The data is plotted for approximately one second after impact. The helicopter originally starts with the impact conditions previously mentioned and both the vertical and lateral velocities finish at 0 m/s (0 ft/s), while the horizontal velocity has not quite reached 0 m/s, indicating the vehicle is sliding for one second after the impact. The vehicle slid and came to rest 13.72 m. (45 ft) away from the impact location, outside the view of the photogrammetry cameras and after the time shown in the figures. The impact and post impact angles also show after the impact the vehicle pitched down to approximately 12 degrees, which can be seen from the image sequence in Figure 5. The vehicle yaw increased after the initial impact, which corresponded to the vehicle turning left during the slide-out. The vehicle roll was unable to be computed past approximately 0.275 s.

Finally, relative deflection between the discrete points on the helicopter was examined. Areas of large relative deflection on the aircraft suggested possible compromises in structural integrity and possible damage. Figure 16 shows the locations and identification of the points, while Table 2 shows the results.

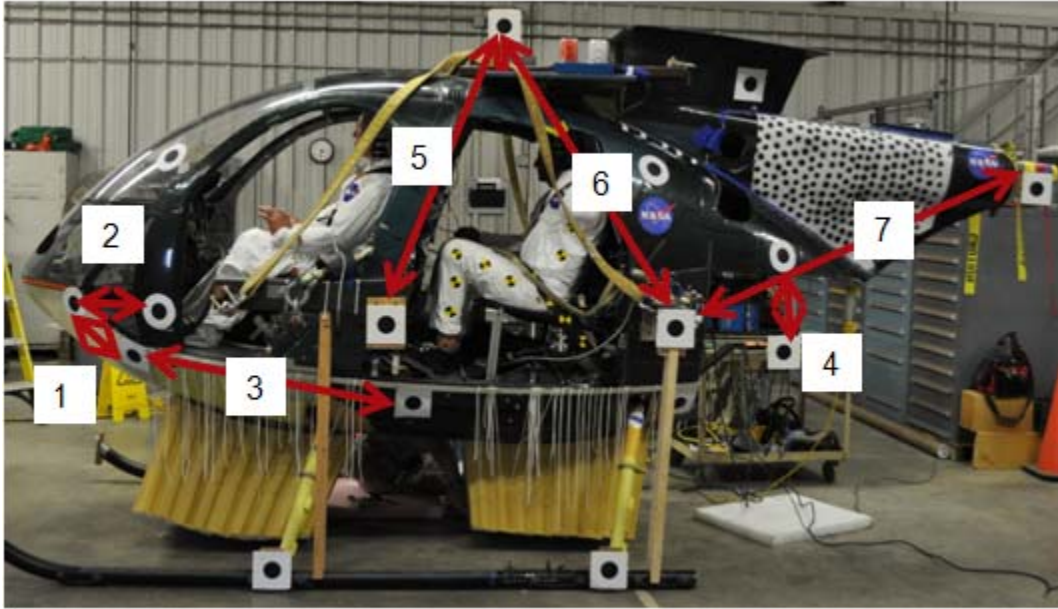


Figure 16 – Vehicle target locations for deformation measurements.

Table 2 – MD-500 Relative Displacements

Vehicle location	Relative Displacement, %
Nose to Water Line (1)	0.85
Seat Line (2)	0.47
Water Line (3)	0.17
DAS Shelf Support (4)	0.98
Top Mass to Front Lifting fixture (5)	0.32
Top Mass to Rear Lifting fixture (6)	0.34
Tail to Rear Lifting fixture (7)	0.24

Table 2 shows the highest relative displacements occurred in the front of the vehicle, and near the rear of the vehicle labeled “DAS Shelf Support”. The relative displacements that occurred in the front of the vehicle were from the nose impacting the surface first due to the pitched down orientation of the helicopter at impact. At impact, the DEA began crushing pushing the nearest targets (located at positions

1 and 2 in Figure 16) upward while the ballast mass in the nose of the aircraft continued at a downward trajectory. However, the photogrammetry showed that there was no permanent deflection, thus the nose rebounded back into place. The other area of high relative deflection was near the rear of the helicopter, under the tail support, in position 4. Position 4 measured the relative deflection on a connection bar between the aircraft frame and a metal plate which held the onboard data acquisition system. The plate with the acquisition system weighed approximately 68 kg. (150 lbs), and was cantilevered from brackets attached to the rear bulkhead. As the helicopter impacted the surface and rebounded, the shelf's momentum caused it to deform the bar or the frame enough to be calculated by the photogrammetry system. However, as with the helicopter nose, the deformation was not permanent and the bar elastically rebounded to its initial position. All other areas examined exhibited low deflection, and confirmed the findings from the visual inspections that the airframe was relatively undamaged.

CONCLUSION

A full-scale crash test conducted on December 2, 2009, successfully demonstrated the feasibility of using the Deployable Energy Absorbing composite honeycomb concept (DEA) for dynamic load attenuation in a realistic crash scenario. DEAs were attached to the bottom of an instrumented MD-500 helicopter, which impacted a concrete surface at a resultant velocity of 14.2 m/s (46.5 fps). The response data shows that the airframe experienced a peak acceleration of approximately 15 g in the vertical and 8 g in the horizontal directions. Airframe deflection data from strain gage rosettes and photogrammetry measurements suggested that the airframe survived the impact relatively undamaged after the impact. The occupant data was processed through various injury criteria, all of which showed no injury.

REFERENCES

- [1] O'Bryan, Thomas C., and Hewes, Donald E., "Operational Features of the Langley Lunar Landing Research Facility." NASA Technical Note, TN D-3828, February 1967.
- [2] Vaughan, Jr., V. L. and Alfaro-Bou, E., "Impact Dynamics Research Facility for Full-Scale Aircraft Crash Testing." NASA Technical Note, TN D-8179, April 1976.
- [3] Jackson, K. E., and Fasanella, E. L., "NASA Langley Research Center Impact Dynamics Research Facility Research Survey." *Journal of Aircraft*, Vol. 41, Number 3, pp. 511-522. 2004.
- [4] Taher, S.T. et al., "A New Composite Energy Absorbing System for Aircraft and Helicopter." *Composite Structures* 75, pp. 14-23, 2006.
- [5] Jones, L. E., and Carden, H. D., "Evaluation of Energy Absorption of New Concepts of Aircraft Composite Subfloor Intersections." NASA TP 2951, November 1989.
- [6] Fasanella, E. L., and Jackson, K. E., "Analytical and Experimental Evaluation of Composite Energy Absorbing Subfloor Concepts." *Proceedings of the AHS National Technical Specialists Meeting on Rotorcraft Crashworthiness*, September 14-17, 1998, Phoenix, AZ.
- [7] Bisagni, C., "Crashworthiness of Helicopter Subfloor Structures." *International Journal of Impact Engineering*, Vol. 27, No. 10, pp.1067-1082. 2002.
- [8] Kellas, S., and Knight, N. F., Jr., "Design, Fabrication, and Testing of Composite Energy-Absorbing Keel Beams for General Aviation Type Aircraft." *Proceedings of the 42nd AIAA/ASME/ASCE/AHS/ASC Structures, Structural Dynamics, and Materials Conference and Exhibit*, AIAA-2001-1529, Seattle, WA, April 16-19, 2001.
- [9] Kindervater, C. M., "Crash Resistant Composite Helicopter Structural Concepts Thermoset and Thermoplastic Corrugated Web Designs." *Proceedings of the American Helicopter Society (AHS) National Technical Specialists Meeting on Rotorcraft Structures*, Williamsburg, VA, October 30-November 2, 1995.

- [10] Desjardins, S.P., "The Evolution of Energy Absorption Systems for Crashworthy Helicopter Seats." *Proceedings of the 59th Annual AHS Forum*, Phoenix AZ., May 6-8. 2003.
- [11] Shane J. S., "Design and Testing of an Energy-Absorbing Crewseat for the F/FB-111 Aircraft." NASA CR-3916, August 1985.
- [12] Bolukbasi A. O., "Active Crash Protection Systems for UAVs," *Proceedings of the 63rd AHS Annual Forum*, Virginia Beach, VA, May 1-3, 2007.
- [13] Yosef V. et al., "Rotorcraft External Airbag Protection System," *Proceedings of the AHS 62nd Annual Forum*, Phoenix AZ, May 2006.
- [14] Tutt B. et al., "A Summary of the Development of a Nominal Land Landing Airbag Impact Attenuation System for the Orion Crew Module." 20th AIAA Aerodynamic Decelerator Systems Technology Conference, Seattle, Washington, 4-7 May 2009.
- [15] Kellas S., "Deployable Rigid System for Crash Energy Management." US Patents 6,755,453, June 29, 2004, 6,976,729 December 20, 2005, and 7,040,658 May 9 2006.
- [16] Kellas S. and Jackson K. E., "Deployable System for Crash-Load Attenuation," *Proceedings of the 63rd AHS Annual Forum*, Virginia Beach, VA. May 1-3, 2007.
- [17] Kellas S. and Jackson K.E., "Multi-Terrain Vertical Drop Tests of A Composite Fuselage Section." *Proceedings of the 64th Annual AHS Forum*, Montreal, Canada. April 29-May 1, 2008.
- [18] Jackson, P. ed. *Jane's: All the World's Aircraft 2008-2009 ed.* Cambridge University Press. Great Britain. 2008.
- [19] Roberts, J., et al., "Computational and Experimental Models of the Human Torso for Non-Penetrating Ballistic Impact." *Journal of Biomechanics*, Vol. 40, pp. 125-136, 2007.
- [20] Polanco, M.A., "Use of LS-DYNA to Assess the Energy Absorption Performance of a Shell Based Kevlar/Epoxy Composite Honeycomb." *Proceedings from the 11th International LS-DYNA Conference*, Dearborn MI, June 6-8, 2010.
- [21] Military Standard, MIL-STD-1290A (AV), *Light Fixed- and Rotary-Wing Aircraft Crash Resistance*, Department of Defense, Washington DC, 20301, 26 September 1988.
- [22] Code of Federal Regulations, Federal Aviation Regulations for Aviation Maintenance Technicians FAR AMT, Part 27 Airworthiness Standard: Normal Category Rotorcraft, 27.562 Emergency Landing Dynamics.
- [23] Brinkley, J.W. et al., "Development of Acceleration Exposure Limits for Advanced Escape Systems." *NATO AGARD Proceedings*, AGARD-CP-472, February 1990.
- [24] Jackson K. E. et al., "Occupant Responses in a Full-Scale Crash Test of the Sikorsky ACAP Helicopter." *Journal of the American Helicopter Society*, Vol 49, No. 2. April 2004.
- [25] Lawrence C. et al., "The Use of Vehicle Acceleration Exposure Limit Model and a Finite Element Crash Test Dummy Model to Evaluate the Risk of Injuries During Orion Crew Module Landings." NASA TM 2008-215198, 2008.
- [26] Littell, J.D., "Large Field Photogrammetry Techniques in Aircraft and Spacecraft Impact Testing." *Proceedings from the Society of Experimental Mechanics Annual Conference*. Indianapolis IN., June 7-10, 2010.